Prepared for Journal of
Chemical Physics,
May 1963

ORIGIN OF OH CHEMILUMINESCENCE DURING THE INDUCTION PERIOD OF THE H_2-O_2 REACTION BEHIND SHOCK WAVES

By F. E. Belles and M. R. Lauver

Lewis Research Center
National Aeronautics and Space Administration
Cleveland, Ohio

ABSTRACT

The intensity and the rate of increase of light emitted by the $OH^+ {}^2\Sigma^+ \rightarrow {}^2\pi$ (0.0) transition were studied during the induction period behind shock waves in 5% H_2 - 95% air mixture. Induction-zone temperatures ranged from about 1100° to 1900° K, and the initial pressure was 10 Torr. A standard lamp was used to calibrate the optical system, so that photomultiplier signals could be transformed to OH^* concentration. The results are interpreted in terms of radical-recombination reactions. It is found that OH^* is formed in the reaction $H + O_2 + H_2 \rightarrow H_2O + OH^*$, and is effectively quenched, in these experiments, only by water. The excitation process is an inefficient reaction, with an average rate constant of 2×10^5 liter^2/mole^2-sec.

Prepared for Journal of
Chemical Physics,
May 1963

ORIGIN OF OH CHEMILUMINESCENCE DURING THE INDUCTION PERIOD OF THE H_2-O_2 REACTION BEHIND SHOCK WAVES

By F. E. Belles and M. R. Lauver

Lewis Research Center
National Aeronautics and Space Administration
Cleveland, Ohio

INTRODUCTION

The combustion of H_2 and O_2 is accompanied by the emission of ultraviolet light, due to the transition of the excited radical OH^* ($^2\Sigma^+$) to the ground state ($^2\pi$). An understanding of the processes leading to this emission is of interest because it would provide further information on the details of the reaction. Such understanding would also be of value in other ways: it might permit use of the emitted light as an indication of the progress of the main reactions; and it would allow quantitative comparisons to be made between induction times measured by following the concentration of ground state OH with absorption spectroscopy,[1] and those measured by the easier method of observing the emitted light.[2]

For many years, evidence (summarized in ref. 3) has accumulated favoring both a thermal and a nonthermal (chemiluminescent) origin of the excited state of OH in the H_2-O_2 reaction. More recently, Kaskan[4] studied the OH^* emission from $H_2/O_2/N_2$ flame gases, in which the concentrations of the free radicals H, O, and OH are in excess of the equilibrium values. He found that the radiation arises from recombination reactions among these excess free radicals. The intensity of emission was found to be proportional to the cube of the ground-state OH concentration (which was measured by absorption), whereas thermal excitation calls for a first-power dependence.

However, this does not mean that the excitation process involves three OH radicals, because in such flame gases H, O, and OH are equilibrated among

themselves by way of rapid reversible bimolecular reactions, even though they are not in equilibrium with the stable products of the flame. As a result, various relations exist among the concentrations of H, O, and OH. Therefore, Kaskan was not able to choose any specific excitation reaction from among the various possibilities that are both energetic enough, and also account for the observed $[OH]^3$ dependence. He pointed out that further progress might be made by studying a system in which the radicals are not equilibrated with each other, providing that methods are available for the separate measurement of each radical concentration.

Schott and Kinsey[1] found that a well-defined, highly nonequilibrium region exists behind shock waves in $H_2/O_2/Ar$ mixtures. After the gas has been compressed and heated by the shock front, there is an induction period during which the H, O, and OH concentrations increase exponentially with time due to chain branching, while the temperature, pressure, and reactant concentrations all remain virtually constant. The induction periods range from a few to a few hundred microseconds over convenient ranges of shocked-gas properties.

As to the concentrations of free radicals, they need not be measured. Instead, they can be calculated with some confidence by integrating the small set of chemical rate equations that govern the branching process during the induction period. The required rate constants are now fairly well established.

Thus, the necessary ingredients for further study of OH^* excitation in the H_2-O_2 reaction are available. This paper describes measurements of OH^* radiation intensity, and its timewise variation, in the induction zone behind shock waves traveling through 2% H_2 - 98% air mixture. The results are interpreted in terms of radical-recombination reactions.

EXPERIMENTAL

The rectangular shock tube (approx. inside dimensions, 37 × 74 mm) is shown schematically in figure 1. It was equipped with a miniature piezoelectric pickup (T) used to trigger an oscilloscope, followed by 6 thin-film resistance gages. Tow of these were upstream of the test section.

Two oscilloscopes were used. On one of them, the outputs of thin-film gages 1, 2, 6, and on occasion, 3, were displayed and photographed. Measurements of the time interval between shock arrival at the various stations gave either two or three velocities, over a tube length of 410 mm. The second oscilloscope had two independent electron beams, and was triggered by gate signals from the first. On one beam, the outputs of gages 4 and 5 were displayed to give a localized velocity measurement over an interval of 63.5 mm. Light emission was displayed on the other beam. Timing signals produced by a crystal-controlled secondary frequency standard were recorded on all three oscilloscope beams for each run. In addition, it was determined that the two traces of the dual-beam oscilloscope were in phase at some known instant during their sweep.

The gas mixture used, 5% He - 95% air, is quite exothermic, so there was concern that the heat release might accelerate the wave as it moved down the tube. This proved to be unfounded, so long as the initial pressure was low. All the tests reported were run at 10 Torr initial pressure; the measured velocities over the entire 410 mm instrumented length were either very nearly constant or slowly decreasing, depending on the Mach number, and showed neither acceleration nor periodic changes.

Two opposite walls of the test section were made of transparent quartz plates, one of which was masked by a metal sheet containing a vertical slit

1 mm wide. This slit was located at the same axial position as thin-film gage number 4. Light emitted through the slit was observed by means of a grating monochromator with its entrance slit set at 1-mm width and located 20 cm away from the window. This arrangement gave very good time resolution. The monochromator viewed radiation from a wedge of gas that had an axial thickness averaging about 1.3 mm; and since the shock speeds were 1.3 mm/μsec or greater, the time resolution was better than 1 μsec. The monochromator passed light in a 33 Å region of the (0,0) band, centered at 3080 Å. The light was detected by a type 1P28 photomultiplier. Figure 2 is a typical record of the dual-beam oscilloscope display, obtained with relatively low gain on the photomultiplier channel. It shows, on the upper beam, the arrival of the shock at thin-film gage number 4 (and at the observation slit), and the subsequent arrival at gage number 5; and on the lower beam, the photomultiplier signal.

The optical system and photomultiplier were calibrated by means of a standard incandescent lamp with known spectral radiance.* It was found that a signal of 1 millivolt corresponded to 7.8×10^{-17} moles/liter of electronically excited hydroxyl radicals. This number was arrived at without any correction for self-absorption, and assumes a constant transition probability of 1.8×10^{6} per second[6] for all rotational lines contained in the observed 33 Å region of the (0,0) band.

RESULTS

Data on intensity of emitted light versus time were read from oscillograms such as figure 2. Zero time is the instant that an element of gas passes through the shock front, and this was fixed by the time of shock

*National Bureau of Standards lamp number U-81.

arrival at thin-film gage number 4. Times measured from the oscillograms were multiplied by the density ratio across the shock to convert them to true gas times. The density, pressure, and temperature ratios were calculated from the measured Mach number by the graphical method of Markstern? In making these calculations, it was assumed that no significant chemical reaction occurred during the induction period, and that the gas reached full thermal equilibrium. The range of shock-wave Mach numbers was about 3.8 to [illegible], corresponding to induction-zone temperatures from about 1100 to 1300° K.

Typical intensity-time data are shown in figure 3, for several temperatures. Oscilloscope voltages have been reduced to concentrations of excited hydroxl radical, $[OH^*]$, by means of the calibration factor. It was found that $[OH^*]$ grown exponentially with time over about 2 observable orders of magnitude increase in $[OH^*]$, after which an inflection occurs and a maximum is reached. It is the early exponential part of the history that is of first interest in the present work. During this period, $[OH^*] \propto \exp(t/\tau)$. The exponential time constants, $1/\tau$ sec^{-1}, were obtained from the slopes of lines such as those shown in figure 3, drawn through the data by inspection.

DISCUSSION

Chain-Branching Process

During the induction period of the H_2-O_2 reaction, the concentrations of the free radicals H, O, and OH grow rapidly by chain branching. The rate of this process is governed by the rates of a few rapid bimolecular reactions. Before these reactions can become effective, however, a small concentration of free radicals must be built up by some initiation process in which molecular species react. At sufficiently high temperatures, the dissociation of hydrogen is no doubt an important means of initiation; but for the range up to 1300° K

covered in the present work, it was assumed that only the following reaction contributes:

$$H_2 + O_2 \rightarrow 2OH \qquad (I)$$

If it is assumed, as Schott and Kinsey[1] did, that the induction period lasts until the concentration of ground-state hydroxyl radicals reaches 10^{-7} moles/liter, then it turns out that the initiation period is only a small part of the induction period. The growth of free-radical concentrations during most of this time is strictly exponential, with a time constant that is greatly influenced by the rate of the slow chain-branching reaction:

$$H + O_2 \rightarrow OH + O \qquad (II)$$

However, if $[H_2]/[O_2] < 1$ as in these experiments, the following reactions also affect the process:

$$O + H_2 \rightarrow OH + H \qquad (III)$$

$$OH + H_2 \rightarrow H_2O + H \qquad (IV)$$

Finally, the following reaction may be included for the sake of completeness:

$$OH + OH \rightarrow H_2O + O \qquad (V)$$

It turns out to be without effect on the results, because even though its rate constant is large, its rate is very small owing to the small values of [OH] that exist during the induction period.

Reactions I - V were used to set up the differential equations describing the growth of [H], [O], and [OH] during the induction period. These were integrated numerically by means of an IBM 7090 program, using the Runge-Kutta method.[8] The rate constants used are listed in table I.

Figure 4 is a semi-logarithmic plot of the calculated quantities for an induction-zone temperature of 1300° K, and is typical of the results for

other temperatures. It is seen that the plots are linear except for a brief initiation period, and that all three lines have the same slope. Therefore,

$$\frac{[H]}{[H]_0} = \frac{[O]}{[O]_0} = \frac{[OH]}{[OH]_0} = e^{t/\tau} \qquad (1)$$

where the concentrations with subscript zero are the values obtained by extrapolation to zero time. The fact that a single time constant τ suffices to describe the growth of all three free-radical concentrations greatly simplifies the prediction of OH^* concentration. Table II lists the pseudo-initial concentrations and the time constants obtained from calculations using two different sets of rate constants from table I.

Production of OH^* by Radical Recombination

In order to excite ground-state OH to the $^2\Sigma^+$ (v = 0) state, 88.3 kcal/mole are required. Therefore, the chemiluminescent production of OH^* can only be accomplished by a few energetic reactions which involve either the transfer of heat of recombination to OH acting as a third body, or the direct production of OH^* in a highly exothermic reaction. The possibilities in the first category are:

$$H + H + OH \rightarrow H_2 + OH^* \qquad (VIa)$$

$$O + O + OH \rightarrow O_2 + OH^* \qquad (VIb)$$

$$H + OH + OH \rightarrow H_2O + OH^* \qquad (VIc)$$

and

$$O + H_2 + OH \rightarrow H_2O + OH^* \qquad (VIIa)$$

In the second category are:

$$O + H + M \rightarrow OH^* + M \qquad (VIIb)$$

and

$$H + O_2 + H_2 \rightarrow H_2O + OH^* \qquad (VIII)$$

The rates of reactions VI involve three free-radical concentration terms; the rates of reactions VII involve two; and the rate of reaction VIII, only one.

In calculating the rate of growth of $[OH^*]$, it is reasonable to include a quenching reaction. It has been found[11,12] that OH^* is very effectively quenched by H_2O. For the present, however, it will be assumed that quenching occurs by the following nonspecific reaction:

$$OH^* + M \rightarrow OH + M \qquad (IX)$$

In view of the results of the calculations of free-radical concentrations, as expressed by equation (1), the growth of $[OH^*]$ is given as follows if the excitation reaction is VIa, b, or c:

$$d[OH^*]/dt = k_e C_3 e^{3t/\tau} - k_q[OH^*][M] \qquad (2)$$

Here, k_e is the rate constant of the excitation reaction, and k_q that of the quenching reaction. The term C consists of the product of three concentration terms; for example, $C_3 = [M]_0^2[OH]_0$ if the excitation reaction is VIa. The subscript 3 denotes the fact that all three terms refer to free-radical concentrations.

Similarly, reactions VIIa and VIIb lead to:

$$d[OH^*]/dt = k_e C_2 e^{2t/\tau} - k_q[OH^*][M] \qquad (3)$$

and reaction VIII leads to:

$$d[OH^*]/dt = k_e C_1 e^{t/\tau} - k_q[OH^*][M] \qquad (4)$$

Integration[13] of equations (2), (3), or (4) yields:

$$[OH^*] = \frac{k_e C_n (e^{nt/\tau} - e^{-k_q[M]t}}{n/\tau + k_q[M]} \qquad (5)$$

in which n may be 1, 2, or 3 depending upon the type of excitation reaction assumed.

Comparison of Observed and Predicted $[OH^*]$

There are two ways in which the experimental data may be compared with the predictions of equation (.). First, the observed OH^* concentrations may be compared in magnitude with the calculated values. Second, the time dependencies may be compared.

Comparison of magnitudes. - It will be appreciated that the calculated value of $[OH^*]$ at a given time during the induction period may vary by several orders of magnitude, depending upon the type of excitation reaction assumed. For instance, figure 4 shows that, at 1500° K, $[H]_0 \sim 10^{-12}$, $[O]_0 \simeq 10^{-11}$, and $[OH]_0 \sim 10^{-12}$ moles/liter. Consequently, if it is assumed that excitation occurs via one of the three-free-radical reactions, VI, then C_3 will be of the order of 10^{-35} at this temperature. On the other hand, if reaction VIIa or VIIb is assumed, C_2 will be of the order of 10^{-27} to 10^{-31} ($[M] \simeq 10^{-3}$, $[H_2] \simeq 10^{-4}$ moles/liter). Although $\exp(2t/\tau)$ is considerably larger than $\exp(t/\tau)$, it is not enough greater to counteract this difference between C_3 and C_2 during the induction period.

It is instructive to calculate upper limits for $[OH^*]$, assuming each of the possible excitation reactions in turn, and to compare the results with observed concentrations. This can be done by assuming that there is no quenching - i.e., $k_q = 0$ - and that $k_c = 1 \times 10^{10}$ liter^2/mole^2-sec, corresponding to a very effective 3-body reaction at 1500° K. Equation (.) then becomes:

$$[OH^*] = \frac{1 \times 10^{10} C_n (e^{nt/\tau} - 1)}{n/\tau} \qquad (.)$$

Figure . shows curves calculated from equation (.), using data from table II(a). Also shown is a line drawn through experimental data obtained at 1407° K.

It is seen that the observed OH^* concentrations lie many orders of magnitude above the values expected for the three-free-radical reactions, VIa, VIb, and VIc. They also may be well above the curves computed for the two-free-radical processes, VIIa and VIIb. Moreover, it should be noted that if OH^* were formed thermally, its concentration would be about $\exp(-88000/RT)$ times the ground-state OH concentration, or about 13 orders of magnitude below the uppermost curve of figure 7. Data for other temperatures behave in the same manner. Consequently, comparison of observed $[OH^*]$ with the maximum values that can reasonably be calculated favors reaction VIII as the one responsible for excitation.

Discussion of the fact that the observed $[OH^*]$ are less than the upper-limit values predicted on the basis of reaction VIII will be deferred to the section on quenching.

Comparison of time dependencies. - If excitation does in fact occur by way of reaction VIII, n should be unity in equation (8). Observed $[OH^*]$ and calculated concentrations of ground-state free radicals, plotted semi-logarithmically against the time, should have the same slope at a given temperature. The extent to which this is borne out is shown in figure 8. The observed time constants are in excellent agreement with the ones calculated using the "best" values of rate constants in table I, up to about 1000° K. At higher temperatures, the data fall progressively farther above the curve. Nevertheless, they are still within reasonable bounds. This is shown by the dashed curve, which was calculated using the upper-limit value for k_3 (table I), i.e., $k_3 = 1.5 \times 10^{10} \exp(-2700/RT)$. It can be seen that a somewhat smaller modification of k_3 would have fit the data better, but no effort was made to optimize the fit.

The uppermost curve of figure 6 shows the exponential time constants that result if only reaction II is important. Schott and Kinsey[1] pointed out that it would be rate-controlling if $[H_2]/[O_2] \geq 1$, and that $1/\tau$ would then be equal to $2k_2[O_2]$. Obviously, the fact that $[H_2]/[O_2] < 1$ in the present experiments has a very large effect on the chain-branching process.

Quenching of OH^*

The discrepancy in figure 5 between the observed $[OH^*]$ and the values predicted on the basis of reaction VIII can be explained by generalized quenching (reaction IX). If it is assumed that k_q corresponds to the collision number, say, 5×10^{11} liter/mole-sec, then the term $k_q[M]$ in the denominator of equation (5) will be much larger than $1/\tau$. Moreover, the term $\exp(-k_q[M]t)$ will be negligible compared to $\exp(t/\tau)$ at all times greater than 1 μsec. Equation (5) then becomes

$$[OH^*] = \frac{k_8[H]_0[O_2][H_2]e^{t/\tau}}{5\times10^{11}[M]} \qquad (7)$$

when written in the form appropriate for reaction VIII. Solving equation (7) for k_8, and inserting experimental data from figure 5 and values of $1/\tau$ and $[H]_0$ from table II(b) yields $k_8 \approx 0.4\times10^{10}$ liter^2/mole^2-sec, corresponding to a very efficient three-body reaction. It is interesting to note that Kaskan[4] reached exactly the same conclusion when he used his light-intensity measurements to deduce k_8, after setting the rate constant for the quenching reaction equal to the binary collision number.

If the picture of the excitation and quenching of OH^* that is embodied in equation (7) is correct, then neither k_8 nor k_q should depend much on the temperature. Values of k_8 calculated from equation (7) by using experimental data should be nearly constant over the whole range of temperatures

from 1100° to 1900° K. But in actual fact these "experimental" k_8's, although they scatter badly, indicate a strong trend with temperature. In order to explain the data, they must be rather greater than 10^{10} liter^2/mole^2-sec at 1100° K, and two or three orders of magnitude less at the upper end of the temperature range.

If, on the other hand, it is assumed that there is no quenching ($k_9 = 0$), the k_8's naturally turn out to be much smaller, but they still have the same strong temperature dependence.

To put the situation another way: the intensity of OH^* emission is unexpectedly small at high temperatures, and unespectedly large at low temperatures. One ready explanation for these facts is that quenching occurs by collisions with a reaction product. The obvious candidate is of course H_2O, which is known to be a very effective quencher from flame studies.[11,12]

Another reason for suspecting that the observed behavior is due to quenching by H_2O is that the light intensity-time traces go through an inflection point quite early. Recent interferometric density measurements by White[14] on low-pressure H_2-O_2 detonations have confirmed that there is no appreciable heat release for times comparable to the induction times of Schott and Kinsey,[1] who identified the end of the induction period with the attainment of $[OH] = 10^{-6}$ moles/liter. In the present experiments at, say, 1500° K, the calculations of table II(b) show that this concentration is reached after about 70 μsec. But near 1100° K, the light-intensity curves go through an inflection at around 45 μsec. If this change in the rate of increase of $[OH^*]$ were merely due to the disappearance of free radicals in the heat-releasing recombination part of the reaction, it should occur closer to 70 μsec. The same thing is found at all temperatures; except perhaps the

very highest ones: namely, the inflection point occurs well before the end of the induction period. This, too, can be qualitatively explained by supposing that the H_2O concentration, which also rises exponentially during the induction period, finally becomes great enough to exert an observable quenching effect.

In order to test this idea quantitatively, it is necessary to derive a new expression for the prediction of $[OH^*]$, assuming that reaction IX is replaced by the following quenching reaction:

$$OH^* + H_2O \rightarrow OH + H_2O \qquad (X)$$

Since H_2O is produced almost solely by reaction IV during the induction period,

$$d[H_2O]/dt = k_4[OH][H_2] = k_4[OH]_0[H_2]e^{t/\tau} \qquad (8)$$

Integrating between limits of 0 and t,

$$[H_2O] = k_4[OH]_0[H_2]\tau(e^{t/\tau} - 1) \qquad (9)$$

Therefore,

$$d[OH^*]/dt = k_8[H]_0[O_2][H_2]e^{t/\tau} - k_{10}k_4[OH]_0[H_2][OH^*]\tau(e^{t/\tau} - 1) \qquad (10)$$

Equation (10) cannot be readily integrated. However, useful results can be obtained from the form of equation (10) that is applicable to times great enough so $e^{t/\tau} \gg 1$. If, for example, this inequality is taken to be satisfied when $e^{t/\tau} = 2$, then using values of $1/\tau$ from table II(b), the inequality holds from 40 μsec on at 1100° K, and from 3 μsec on at 1400° K. It will be assumed that the form of equation (10) obtained by dropping the factor of unity in the second term on the right-hand side applies to the region in which the inflection point occurs. Differentiating and setting the result equal to zero, one obtains:

$$t_{infl} = \frac{2.303}{1/\tau} \log_{10}\left(\frac{(1/\tau)^2}{k_{10}k_4[OH]_0[H_2]}\right) \qquad (11)$$

and

$$k_8 = \frac{k_{10}k_4[OH]_0[OH^*]_{infl}}{1/\tau[H]_0[O_2]} \qquad (12)$$

It is seen that equation (11) permits the time at which the inflection point occurs to be calculated without recourse to any experimental data. This has been done, using the data from table II(b) and assuming k_{10} is the collision number. The results are plotted in figure 7. Experimental inflection times were estimated directly from the photomultiplier records and multiplied by the density ratio across the shock to convert from laboratory to gas time. The data points plotted in figure 7 include those from the runs used to obtain intensity-time data, and also those from a large number of runs made to measure induction times; in the latter, the oscilloscope gain was too small to give detailed intensity-time data in the early part of the induction period, but the inflection point could be read. All in all, the observed times agree well with those predicted by means of equation (11). Although the points tend to drift away from the curve at the higher temperatures, this may partly be due to the fact that the approximation used ($e^{t/\tau} \gg 1$) becomes worse at these temperatures.

Finally, equation (12) was used to estimate values for k_8. Once, again, the data from table II(b) were used, and k_{10} was taken as the binary collision number. The concentration of OH^* at the inflection point could be read to within a factor of about two at the higher temperatures, more closely at the lower ones. In contrast to the calculations of k_8 made with the previously discussed assumptions about the quenching, the calculations made with equation (12) produced much more nearly constant values. The range of k_8 was 4×10^4 to 9×10^5, with no discernible temperature dependence. The average for

23 runs in which [OH^*] could be read at the inflection point was 2×10^{-9} liter^2/mole^2-sec.

Thus, the data make sense when viewed with the idea that OH^* is effectively quenched only upon collision with H_2O. This treatment leads to a rate constant for the excitation reaction that corresponds to an inefficient process, with a steric factor of about 10^{-5}. Since the excitation reaction VIII involves extensive re-arrangement of bonds, it is very reasonable that it should be an inefficient process.

CONCLUSIONS

The formation of electronically-excited hydroxyl radical during the induction period behind shock waves in 2% H_2 - 98% air mixture occurs via the three-body reaction

$$H + O_2 + H_2 \rightarrow H_2O + OH^*$$

The rate of increase in OH^* concentration during the early part of the induction period can be successfully predicted by using literature values for the rate constants of the chain-branching reactions.

The data indicate that OH^* is effectively quenched only by H_2O in these experiments, and that the excitation reaction is an inefficient one, with a rate constant averaging 2×10^{9} liter^2/mole^2-sec over the temperature range from about 1100° to 1300° K.

REFERENCES

1. G. L. Schott and J. L. Kinsey, J. Chem. Phys. 29, 1177 (1958).

2. H. Gg. Wagner, 9th Symposium (International) on Combustion, p. 444. (Academic Press, Baltimore, 1963.)

3. K. J. Laidler, The Chemical Kinetics of Excited States. (Clarendon Press, Oxford, 1955.)

4. W. E. Kaskan, J. Chem. Phys. 31, 944 (1959)

5. F. Kaufman and F. P. Del Greco, 9th Symposium (International) on Combustion, p. 659. (Academic Press, Baltimore, 1963.)

6. T. Carrington, J. Chem. Phys. 31, 1243 (1959).

7. G. H. Markstein, A.R.S. Jour. 29, 588 (1959).

8. J. B. Scarborough, Numerical Mathematical Analysis. (The Johns Hopkins Press, Baltimore, 1930.)

9. R. E. Duff, J. Chem. Phys. 28, 1193 (1958).

10. R. R. Baldwin, 9th Symposium (International) on Combustion, p. 607. (Academic Press, Baltimore, 1963.)

11. H. P. Broida and T. Carrington, J. Chem. Phys. 23, 2202 (1955).

12. T. Carrington, J. Chem. Phys. 30, 1087 (1959).

13. G. M. Murphy, Ordinary Differential Equations and Their Solutions, p. 288. (D. Van Nostrand Co., Inc., Princeton, N.J., 1960.)

14. D. R. White, General Electric Research Lab. Report No. 63-RL-3289C, April 1963.

TABLE I. - RATE CONSTANTS,

$k_i = A_i \exp(-E_i/RT)$,

liters/mole-sec

Reaction	$\log_{10} A_i$	E_i, kcal/mole	Ref.
I	11.0	70.0	9
II	11.3	16.6	10
III	9.4±0.7	7.7±1.0	5
IV	10.8±0.7	8.8±1.0	5
V	9.9±0.3	1.0±0.5	5

TABLE II. - CALCULATED PARAMETERS DESCRIBING FREE-RADICAL CONCENTRATIONS DURING INDUCTION PERIOD. INITIAL PRESSURE, 10 TORR

Shocked-gas		$[H]_0$, moles/liter		$[O]_0$, moles/liter		$[OH]_0$, moles/liter		$1/\tau$, sec^{-1}	
Temperature, °K	Pressure, atm	(a)	(b)	(a)	(b)	(a)	(b)	(a)	(b)
1100	0.2307	3.16×10^{-15}	2.12×10^{-15}	4.38×10^{-15}	1.55×10^{-15}	3.98×10^{-16}	2.82×10^{-16}	2.5×10^{4}	3.9×10^{4}
1300	0.2930	1.82×10^{-13}	1.02×10^{-13}	3.03×10^{-13}	1.19×10^{-13}	3.89×10^{-14}	2.74×10^{-14}	6.3×10^{4}	10.4×10^{4}
1500	0.3838	3.10×10^{-12}	1.89×10^{-12}	1.00×10^{-11}	2.72×10^{-12}	1.24×10^{-12}	7.93×10^{-13}	12.2×10^{4}	20.4×10^{4}
1700	0.4193	3.04×10^{-11}	1.70×10^{-11}	1.03×10^{-10}	3.10×10^{-11}	1.75×10^{-11}	1.00×10^{-11}	18.3×10^{4}	33.9×10^{4}
1800	0.4873	1.80×10^{-10}	9.10×10^{-11}	7.73×10^{-3}	2.00×10^{-10}	1.34×10^{-10}	7.48×10^{-11}	27.4×10^{4}	49.8×10^{4}

[a] Best values for k's, table I.

[b] k_1, k_2, k_4, k_5 best values; $\log_{10}A_3 = 10.1$, $E_3 = 8.7$.

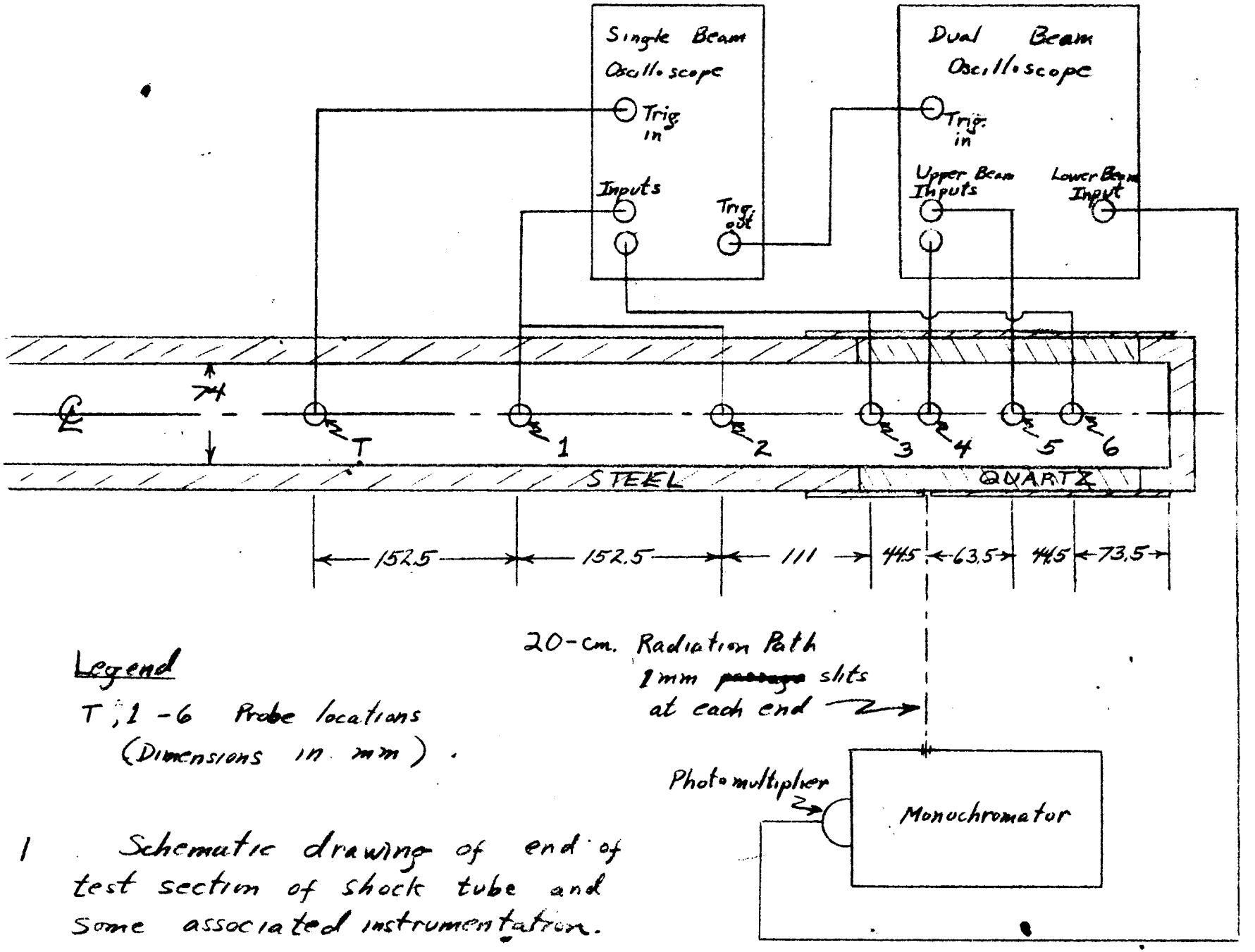

Legend

T, 1 - 6 Probe locations

(Dimensions in mm).

Fig. 1 Schematic drawing of end of test section of shock tube and some associated instrumentation. Top view.

Figure 2 - Typical Oscilloscope Record

Fig 3 - Growth of Excited Hydroxyl Radical Concentration During the Induction Period

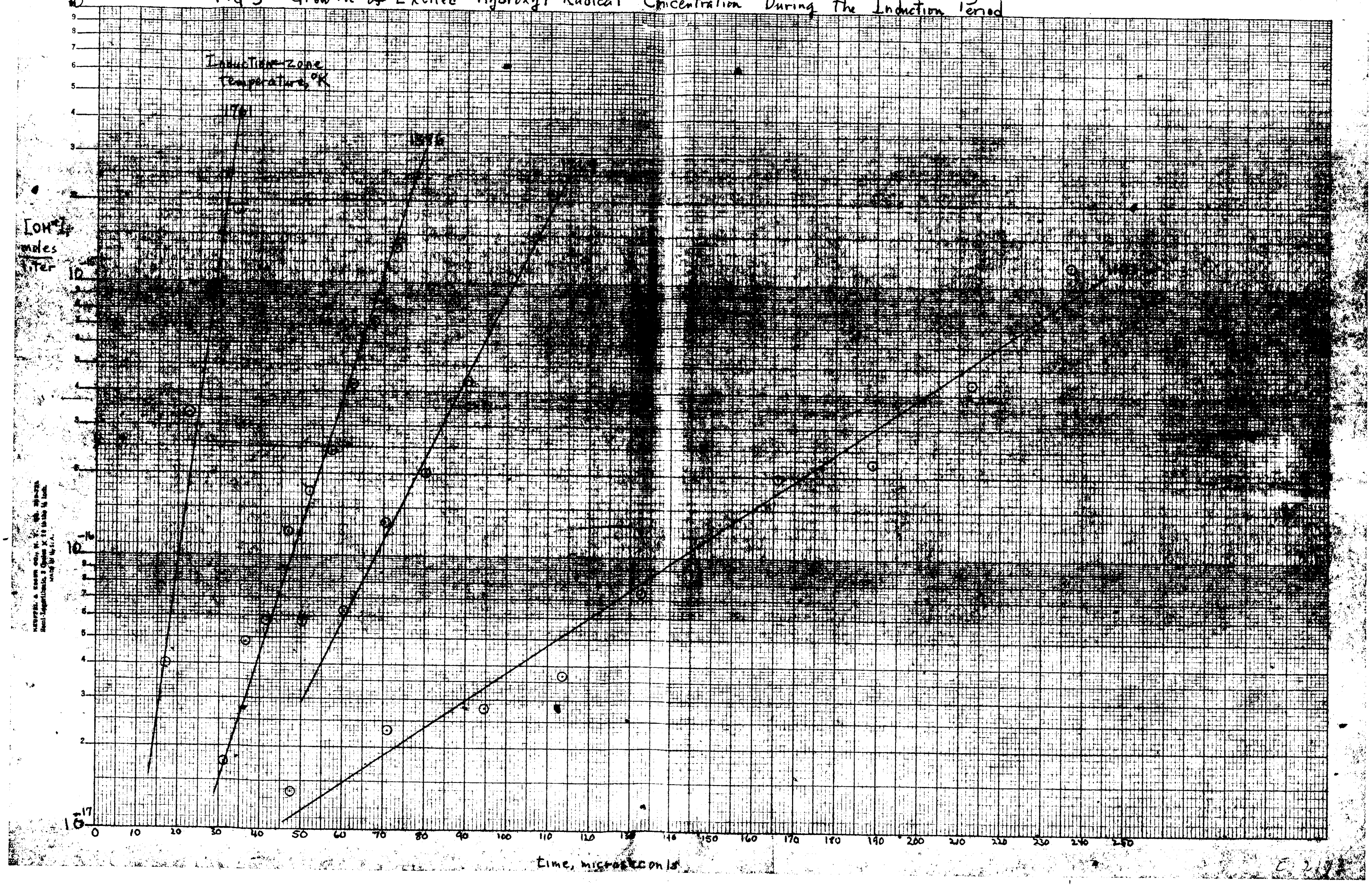

Fig. 6 — Comparison of observed and calculated exponential time constants for growth of [OH*]

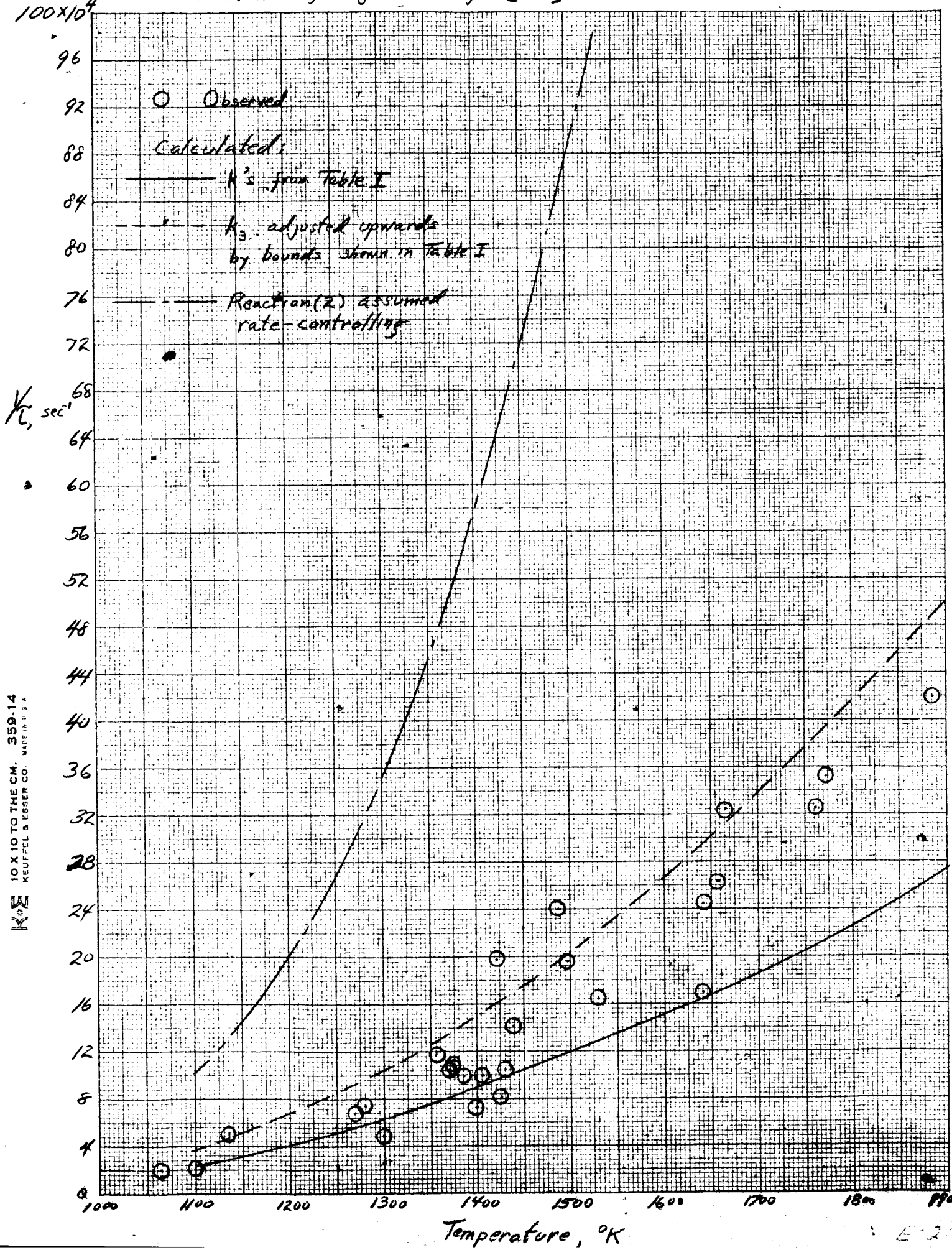

K•E SEMI-LOGARITHMIC 359-64
KEUFFEL & ESSER CO. MADE IN U.S.A.
2 CYCLES X 200 DIVISIONS

FIG. 7 – Comparison of Observed and Predicted Time of Inflection Point in OH^* Concentration

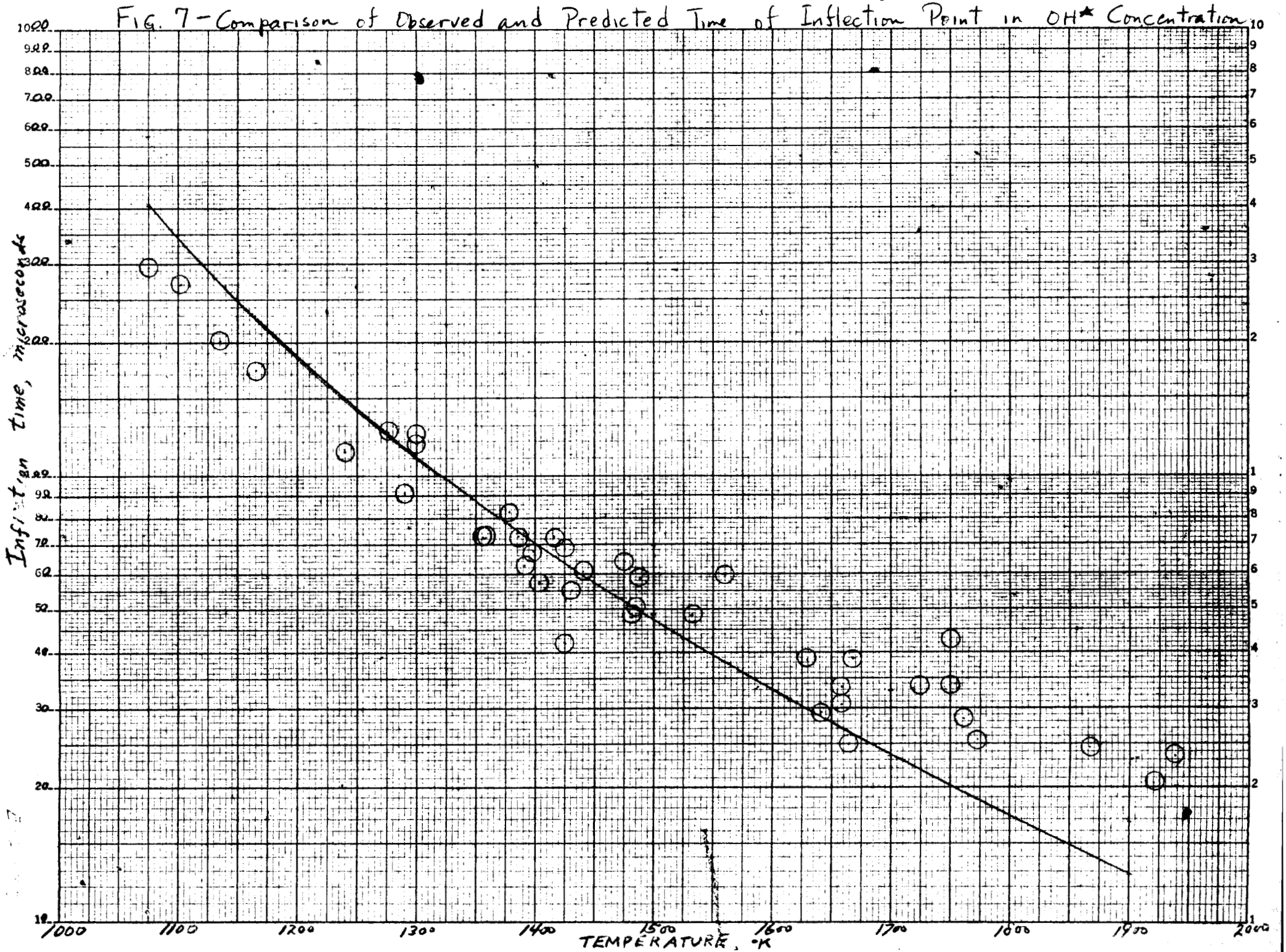

FIG. 4.- Calculated concentrations of ground-state free radicals during the induction period in 5% H_2-95% air. Temperature, 1500°K; initial pressure, 10 Torr.

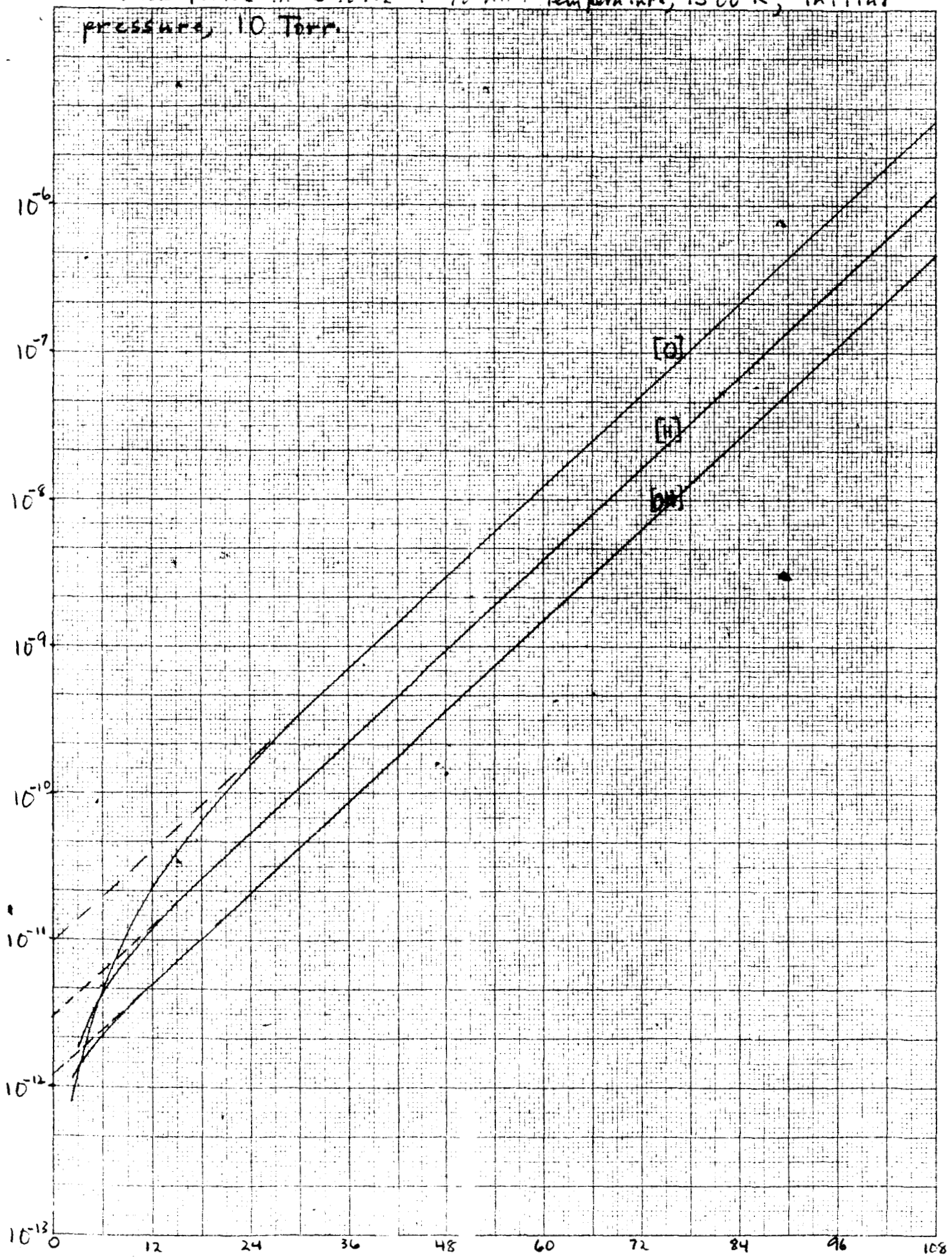

Fig. 5 - Calculated and observed [OH*] during the induction period in 5% H_2 - 95% air. Temperature, 1500°K; initial pressure, 10 Torr.